

Elaboration of the Land use Land Cover Plan of the Subdivision of Monatele in Cameroon

Bikie Gerald Anicet^{1*}; Dongmo Hile Bertrand²; Aba Nkasse Alain²

Elime Boubouama Aime²; Berka Afofeyuf Christian² Mohammed Achab¹

¹Scientific Institut , Mohamed V University, Avenue Ibn Batouta, Rabat Morocco

²National Advance School of Public Works Yaounde Cameroon

Corresponding Author:- Bikie Gerald Anicet^{1*}

Abstract:- Over the past years, humans have directly or indirectly affected the Earth's surface through various activities. These changes in terrestrial ecosystems are closely linked with the issue of the sustainability of socio-economic development since they affect essential parts of our natural capital such as climate, soils, vegetation, water resources and biodiversity. Land Cover has undergone several changes in Cameroon since its independence in 1960. One of the major drivers of this change is urbanization. Uncontrolled, rapid urbanization has had many negative impacts on the center region of Cameroon, around the continuum of its headquarter and in Cameroon metropolises such as anarchical constructions, pollution and traffic congestions. Faced with these urbanization issues, planners need to know the spatiotemporal trends of Land Use Land Cover for the past, present and have predictions of possible future patterns in order to better orient their planning. This is possible through the establishment of Land Use Land Cover maps. Remote sensing and Geographic Information Systems represent a cost-effective method for accomplishing this. In this work, we examine the case of Monatéle, a growing city around the Yaoundé metropolis. Satellite images from 2010, 2017, 2022 were downloaded and classified into five classes using the Support Vector Machine algorithm of image classification. It was found that between 2010 and 2022, settlements have increase continuously from 1.61% to 4.28%, water has decreased continuously from 9.81% to 6.72%, forest has experienced a net decrease from 73.77% to 68.25%, agriculture has experienced a net increase from 12.44% to 16.92%, while Bare Land has had a net increase from 2.38% to 3.82%. of the total surface area of the subdivision of Monatéle. Predictions made for 2029 and 2035 show that by 2035, settlements would have increased to 6.58%, water would have decreased to 4.58%, forest would have decreased to 61.22%, agriculture will take 25.19%, and bare land would have almost remained unvaried, taking up 2.43% of the surface area from 2010 to 2035. This will represent for Monatéle an increase in anarchical settlements, an increased loss in biodiversity, an increased pollution, an increase in demand for basic commodities, and an increased pressure on natural resources, if no planning measures are put in place, though it may represent an increase in human capital,

an increase in local employment opportunities, a reduction of groceries expenditures.

Keywords:- Land use Land Cover, Support Vector Machine, Remote Sensing, Geographical Information Systems, Urbanization.

I. INTRODUCTION

Over the past years, humans have directly or indirectly affected the Earth's surface through various activities. Land use changes are cumulatively transforming Land Cover at an accelerating pace (Turner et al., 1994; Houghton, 1994). These changes in terrestrial ecosystems are closely linked with the issue of the sustainability of socio-economic development since they affect essential parts of our natural capital such as climate, soils, vegetation, water resources and biodiversity (Mather and Sdasyuk, 1991). Today, there is increased recognition that land use change is a major driver of global change, through its interaction with climate, ecosystem processes, biogeochemical cycles, biodiversity and even more importantly human activities (IGPB/IHDP). Changes in ecosystems and livelihood support systems are easily detected by studying Land Use and Land Cover (LULC) changes (Gilani et al., 2014). Understanding the complexity of Land Use and Land Cover changes, its assessments, and monitoring are very important for sustainable management of natural resources, environmental protection, town planning, and food security. (Drummond et al., 2012, Foley et al., 2009, Garedew et al., 2009, Jin et al., 2014). Studies of LULC changes also help in predicting likely future trends and make decisions for the better management of natural resources. (Fan et al., 2007, Gilani et al., 2014, Prenzel., 2004).

Land use and Land Cover in Africa, and more precisely in Cameroon have undergone many transformations. Since independence in 1960, agriculture has been tagged the main driver of these changes in Cameroon, which started as far back as the 1970s when the policy of five-year development plan was launched. It also stands out as the primary driver of deforestation in most sub-Saharan African countries. Agricultural activities are the main causes of land degradation, transforming initial forestlands into agrarian lands in addition to fuel wood activities. In Cameroon, from 0.01 % between 1990 and

2000, forest degradation rate has multiplied by 9 between 2000 and 2005 (Tchindjang et al., 2020). Within the last three decades it has been aggravated by extractive activities and urbanization. Urbanization is a process of political and economic power because the construction of any city is a translation and a reflection of both, for the city appears as a crossroads of trade, enrichment center, tourism, industrialization. Urbanization by threatening biodiversity and raising pressure on land tenure, is an important element in LULC modelling. Because of globalization and modernization, it becomes the main underlying factor of LULC changes in many African cities. Transformations speed up urbanization, which has become one of the biggest challenges in Africa with over 400 million Africans (40% of the population) living nowadays in urban areas, and according to UN Habitat, they will be 60% in 2050. By 2025, while 61% of the world population will live in urban areas, Lagos and Kinshasa will become, according to UN-Habitat, the 11th and 12th largest cities in the world. By now, Kinshasa especially, is expected to have grown by 4 million (an increase of 46%) from 8.7 to 12.7 million between 2010 and 2020. At the same time, Yaoundé is expected to have reached 4-5 million. Thus, urban sprawl with demographic growth and migration is the main factor causing global changes and the primary deforestation driver in the studied region. Around the Yaoundé metropolis and along its continuum, massive expansion of cultivated land, settlements and infrastructure developments occurred at the expense of forests since 1990 (Tchindjang et al., 2020). Uncontrolled, this rapid urban growth has had many negative impacts in and around Yaoundé and in other Cameroonian metropolises such as air, water and land pollution, noise pollution, anarchical land settlements, destruction of flora and fauna, traffic congestion, land conflicts as in the Northern regions between the nomads and the farmers and in the mining zones of East region. Faced

with this urbanization issues, the planners need to know trends of land use in the past, Present and have predictions of possible future land use patterns for growing metropolises, in order to better orient their planning, otherwise growing metropolises will not be any different from established ones. This is possible through the establishment of LULC maps. In this study, we shall examine the case of Monatéle, the headquarter of the Lékié Division, a rapidly growing city in the Centre Region of Cameroon. Our objectives will be to establish the present LULC plan of the Subdivision and using past trends, provide predictions of future LULC patterns to help planners in Monatéle better orient their planning. The study shall consist of the materials and methods employed in which shall be detailed the tools and techniques which shall be applied to carry out the study, results and discussion in which shall be explained the results obtained from the applying the concepts through discussed techniques and a conclusion.

II. METHODOLOGY

Monatéle is a town and a commune in Cameroon, created on the 20th of June 1964, and the capital of the Lékié Division of the Centre Region since 1968. It is located geographically at Latitude 4°10' and longitude 11°45'. According to the 2005 Population Census, the commune of Monatéle had a population of 36,933 inhabitants, including 10,324 in the town of Monatéle itself. The commune of Monatéle is found at about 90Km away from Yaounde, covering a surface area of about 155,4Km² and is confined; northward by the Subdivision of Ebebeda, north-eastward by the subdivision of Sa'a, eastward by the subdivision of Obala, south-westward by the subdivision of Evo doula and the Nyong and Kellé division, and Westward by River Sanaga.

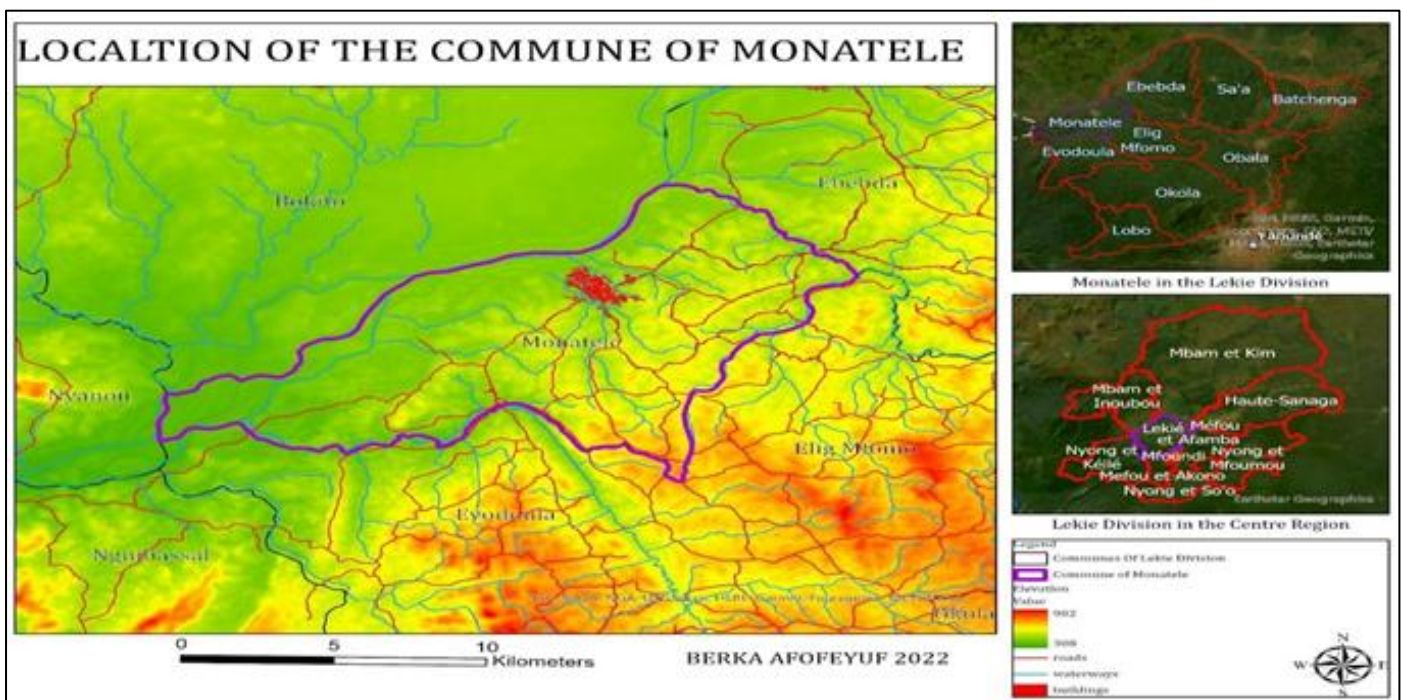


Fig 1 Location of Site of Studies

➤ *Data used*

Satellite images are rich, and provide and play an important role in geographic information provision. Three (03) different satellite images were downloaded from three different time zones in order evaluate the LULC change in the past years, at a time difference of averagely 6 years each, from 2022, 2017, and 2010. This equally helped to make future projections by evaluating the past changes from these

images. Equally, a DEM image was downloaded for elevation data. The period of data acquisition is very important and so the satellite images were acquired in the dry season when the cloud cover is low.

The different image characteristics are presented in the table below.

Table 1 Satellite Image Characteristics

Image Data	Characteristics	Acquisition Date	Source
SRTM (DEM)	Digital élévation data Résolution 30x30m Sensor OLI-TIRS	2019	https://gisgeography.com/usgsearth-explorer
Landsat 8	Planimetry data Resolution 30x30m Sensor OLI-TIRS	2022, 2017	https://gisgeography.com/usgsearth-explorer
Landsat 7	Planimetry data Resolution 30x30m Sensor ETM+	2010.	https://gisgeography.com/usgsearth-explorer

We equally require vector data sets in shapefile formats likes roads, railways, rivers, houses or buildings, geological zone delimitations, administrative boundaries and so on. These datasets were downloaded from Planet.osm, and administrative boundaries from the GIS course of the National Advanced School of Public Works Yaoundé acquired in the year 2021.

➤ *Image Preprocessing*

Pre-processing of satellite images prior to image classification and change detection is very essential. Pre-processing commonly comprises a series of sequential operations, including atmospheric correction or normalization, band ratio, layer stacking, image registration, geometric correction, image enhancement and masking (e.g., for clouds, water, irrelevant features) to correct the surface features reflectance characteristics (El-Kawy et al., 2011; Muriithi, 2016; Kogo et al., 2019; Langat et al., 2019). Some Landsat satellite images and mainly those of ETM+ (Enhanced Thermic Mapper plus) sensors have a lack of information due to satellite scanning errors. These errors result in loss of information which does not allow us to make a good estimate of the different changes that may have taken place, hence the need to correct them. The missing lines are usually 'corrected' by replacing each line with the pixel value of the row above or below it, or with the average or mean of both which is what used in this work. These corrections were carried out in ERDAS IMAGINE 2022 with number of iterations ranging from 7 (band 1 to 7) to 16 (Band 8). In order to save time and ease the pre-processing, the Area of Interest was extracted from all the bands combined in QGIS using the Semi-Automatic Classification Plugin. 'Nodata' areas were also cleared using QGIS' OSGeo4W Shell command prompter.

Satellite sensors used by Earth observation satellites capture the luminance reflected by the earth and the atmosphere from the sun. When the atmosphere is cloudy, the light reflected is no longer just that from the surface of the earth only, but also comprises that reflected by the clouds. The satellite therefore receives a composite of two signals; that from the visible part of the earth and that from the cloudy atmosphere. The latter needs to be removed so that we have just the former, which constitutes the object of our study; the earth's surface. This constitutes therefore the objective of these corrections. For Landsat images, radiometric corrections were carried out to remove the influence of the atmosphere, and then, all the images were converted from digital number (DN) values to top-of-atmospheric (TOA) reflectance to make them comparable. By converting raw DN values to TOA and surface reflectance the atmospheric impacts on the reflected wavelengths are removed so that we can derive the desired indices to use. This was done band after band and then the bands were composed to corrected images with all the bands present for the different color compositions. The first step in the radiometric correction process is to calculate for each image the reflectance of the pixels at the TOA. This step makes it possible to obtain, for the same spectral band, physical measurements which are independent of sensor characteristics.

➤ *Image Classification*

Satellite image classification helps in identifying and extracting details of a given entity in a remote area. It involves grouping image pixel values into meaningful categories. The main reason for undertaking an image classification is, in effect, to convert the image's information on the spectral response of the Earth's surface into a thematic map depicting classes of interest such as land cover. Three broad methods of satellite image classification

exist; automatic, manual, and hybrid, each having its own advantages. The automatic classification method is divided into two different methods, supervised and unsupervised. Supervised classification contains Artificial Neural Network, Support Vector Machine (SVM), Maximum Likelihood, minimum distance, K-nearest neighbor, Binary decision tree, Image Segmentation, Parallelopiped, etc. Unsupervised classification contains the KMeans, ISO data, and so on. The automatic classification method with supervision was used for this work. The satellite image processing and land cover classification was carried out using the accurate Support Vector Machine (SVM) algorithm. The SVM algorithm better classifies validation areas because of the advantage of vector samples which allow a clearer separation of the established classes and thus avoiding confusion (José and Beatriz 2018). SVMs are adaptable and efficient in a variety of applications because they can manage high-dimensional data and nonlinear relationships. The main objective of the SVM algorithm is to find the optimal hyperplane in an N-dimensional space that can separate the data points in different classes in the

feature space. The hyperplane tries that the margin between the closest points of different classes should be as maximum as possible. The SVM was used because it is more accurate than the widely used Maximum Likelihood Classification algorithm. (José and Beatriz, 2018; Abbas et al., 2015). The supervised classification allowed us to define AOIs that identify and recognize features on the image. The classification was performed through identification of features and selection of training areas, evaluation and analysis of training signature statistics and spectral patterns, and classification of the images. The collection of number of training samples and their high representativeness is a critical task for image classification of LULC (Lu and Weng, 2007). For training and validation sampling, Google Earth images and band Combinations were applied for clear identification. The AOIs (training samples) were collected for the various LULC categories, based on knowledge of the area, and uniformity in appearance. Five main LULC class categories were identified and mapped. That is, settlement land, cleared or agricultural land, forest, Bare Soil and water bodies as described in the table below:

Table 2 LULC Classification Classes used for the Images

N°	LULC Class	Description	Color	Class Value
1	Settlement	This includes residential, industrial, and commercial sites, artificial structures and streets.	Mars Red	10
2	Cleared or agricultural land	These are areas with no or only few individual trees, used as pasture or agriculture land, and barren land. This also includes wet and muddy areas, swamps, frequently inundated grass and shrubland, and mangroves.	Yucca Yellow	40
3	Forest	This includes forests patches with closed canopy. This could be deciduous, evergreen or mixed forest land	Leaf Green	30
4	Bare soil	This includes sand dunes, beaches, construction areas, sand and gravel open pit mines, exposed rocks and top soil.	Raw Umber	50
5	Water	Including fresh, brackish and saline water bodies and all other water bodies.	Moorea Blue	20

➤ *Accuracy Assessments*

In remote sensing, accuracy assessment is mandatory in providing information about the quality of the produced classification (El-Kawy et al., 2011). It is essential for individual image classification generated from any remote sensing data (Congalton and Green, 2009). Classification accuracy is the main measure of the quality of thematic maps produced and required by users, typically to help evaluate the fitness of a map for a particular purpose. The accuracy of image classifications has also been central to studies that have sought to evaluate different classification approaches and a suite of issues connected with class discrimination. Although seemingly a simple concept, classification accuracy is a very difficult variable to assess and is associated with many problems (Foody 2002). An error or a confusion matrix is the most frequently used methods and standard form of reporting site-specific classification errors (El-Kawy et al., 2011). In principle, this matrix provides a simple summary of classification accuracy and highlights the two types of thematic error that may occur, omission and commission. This not only summarizes the accuracy of the classification but also may convey useful information to enhance analyses based on the classification (e.g, Prisley and Smith 1987, Fang et al. 2006). The

accuracy assessment was performed on the resulting classified images by generating a set of 115 accuracy assessment points on ArcGIS Pro, converting them to KML, importing and comparing them with actual points on site using google earth pro high-resolution images of the different years in which the Landsat images were downloaded through their class values, thanks to google earth pro’s time slider and site search also during site visit phase. The LULC classification assigned to each pixel was compared with the same location on the reference sources to check whether the classification result is accurate or not on google earth pro and on the field a sample of these points were verified and the ground truthing table used to generate the classification accuracy was filled. Kappa statistic was performed to measure the extent of classification accuracy. The Kappa coefficient is an index to express the accuracy of an image classification used to produce a thematic map (Rosenfield and Fitzpatrick-Lins, 1986). A Kappa coefficient of 90% may be interpreted as 90% better classification than would be expected by random assignment of classes (unsupervised classification). A Kappa coefficient $k < 0.4$ gives poor classification, $0.4 < k < 0.5$ is fair, $0.5 < k < 0.7$ is good, $0.7 < k < 0.85$ is very good, while $k > 0.85$ is excellent according to Moriasi et al.

Table 3 Kappa Coefficient Agreement (Moriasi et al., 2007)

N°	Kappa Coefficient	Level of Agreement
1	<0.4	Poor
2	$0.4 < k < 0.5$	Fair
3	$0.5 < k < 0.7$	Good
4	$0.7 < k < 0.85$	Very Good
5	$k > 0.85$	Excellent

A confusion matrix was created to derive overall user and producer accuracies, and the Kappa statistic using the observed and classified LULC classes of each pixel of the accuracy assessment points.

Land Use Land Cover Change Detection and Analysis

Post-classification change detection technique was applied to compare and analyze the LULC maps resulting from the integration of the results of visual interpretation and supervised classification. Images of different reference years were first independently classified and then the classified images were compared in two periods (2010-2017, and 2017-2022) to detect the differences between each pair of LULC maps. Moreover, overlay procedure and a two-way cross-matrix were used to describe the key change types. Cross tabulation analysis was conducted in order to determine the quantitative conversions from a particular LULC class to another and their corresponding area over the evaluated period on pixel-to-pixel basis using the pixel count. Thus, a new thematic layer was produced from the two five-class maps, containing different combinations of ‘‘from-to’’ change classes. Accordingly, two change maps were produced to display the specific nature of the changes between the classified images. The rate of change was

calculated for each LULC class. The LULC conversion matrix between 2010-2022 was generated and compiled in a matrix table by comparing image values of one data set with the corresponding value of the second data set in each period. The change detection was performed using ArcGIS Pro’s Change Detection Wizard, using a guided workflow of three steps; configure, class configuration and output generation.

➤ Prediction of Future LULC Patterns

A forecast of future LULC patterns was done by the application of Cellular Automata Markov (CA-Markov model) in Idrisi 17.02, the Selva version. CA-Markov is a robust model in predicting the patterns and spatial arrangements of different LULC Change categories. The model operates with respect to historical LULC status change image, a transition probability matrix, and suitability images as a group file. The model is very realistic and comprises two components, the Cellular Automata Model and the Markov Model.

Based on the LULC change trends between 2010 and 2017, a forecast of 2022 LULC was done and the accuracy of the forecast evaluated using the 2022 image classified earlier. Model validation was performed by comparing the simulated 2022 LULC map which was based on 2010 and 2017 classified maps, with the 2022 classified map. The Relative Operating Characteristic (ROC) and Kappa Indices were used to compare agreements between the simulated and classified 2022 LULC maps. The Kappa Indices used included the Kappa for no information (Kno), Kappa for Location (Klocation), Kappa for location Stratum Level (KlocatioStrata) and Kappa for Standard (Kstandard).

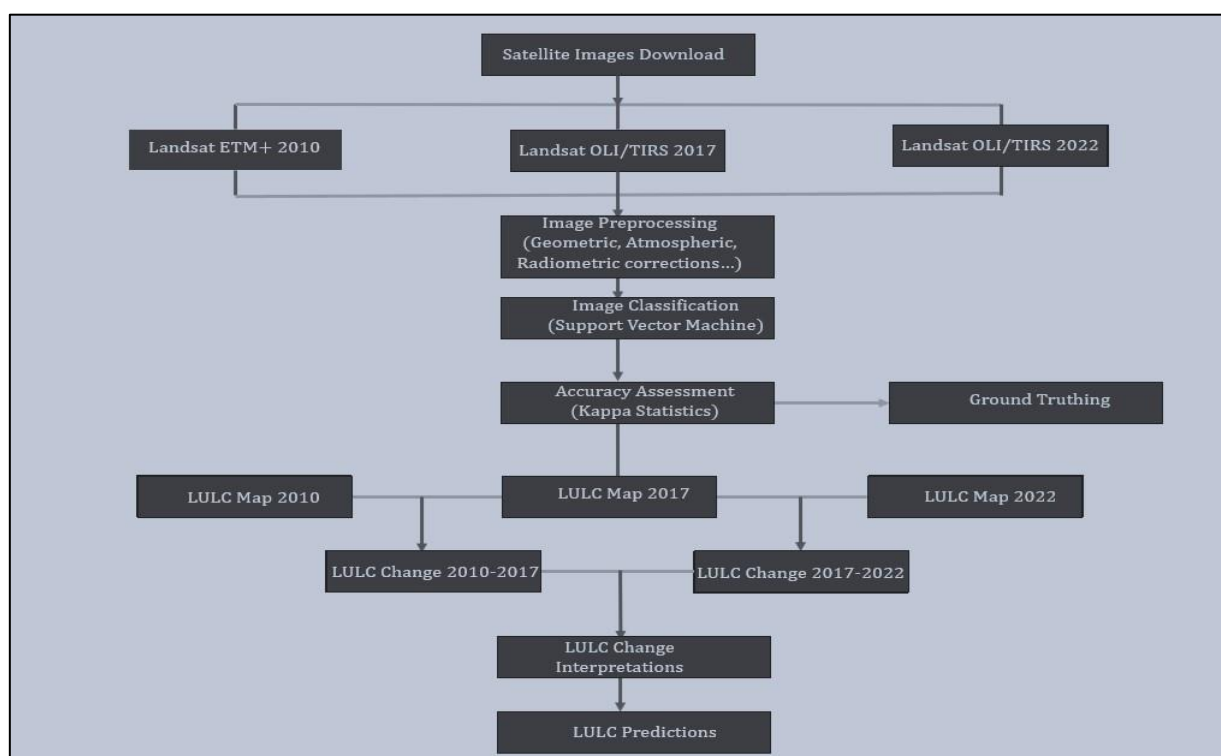


Fig 2 Workflow Diagram

III. RESULTS AND DISCUSSIONS

➤ *Image Classification*

In a total of 15541 Hectares of that make up the commune of Monatéle, in 2010, Forest covered 11464 ha (73.77%), Agriculture Land covered 1933 ha (12.33%), Water covered 1524 ha (9.81%), Bare Land covered 369 ha (2.38%), while settlements covered 250 ha (1.61%). In 2017 9752 ha (62.75%) were covered by Forest, 3777 ha (24.30%) were covered by Agriculture Land, 1152 ha (7.41%) were covered by water, Settlements covered 480 ha (3.09%), while Bare Land covered 380 ha (2.45%) of the total surface area. Classifying the image of 2022 revealed that in a total of 15541 Hectares, forest covered 10606 ha (68.25%), Agriculture Land occupied 2630 ha (16.92%), Water occupied 1045 ha (6.72%), Settlements occupied 666 ha (4.28%), while Bare land Occupied 594 ha (3.82%). These results are illustrated in the Figures below.

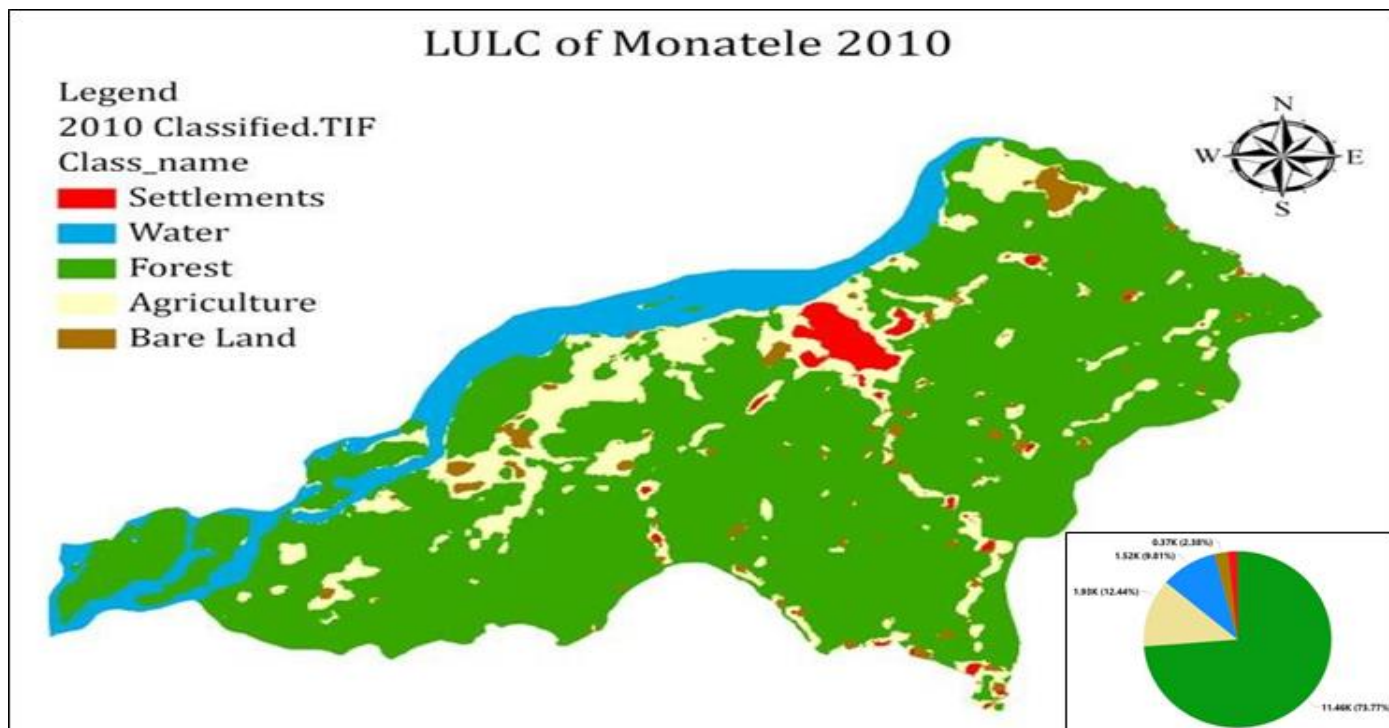


Fig 3 LULC of Monatéle in 2010

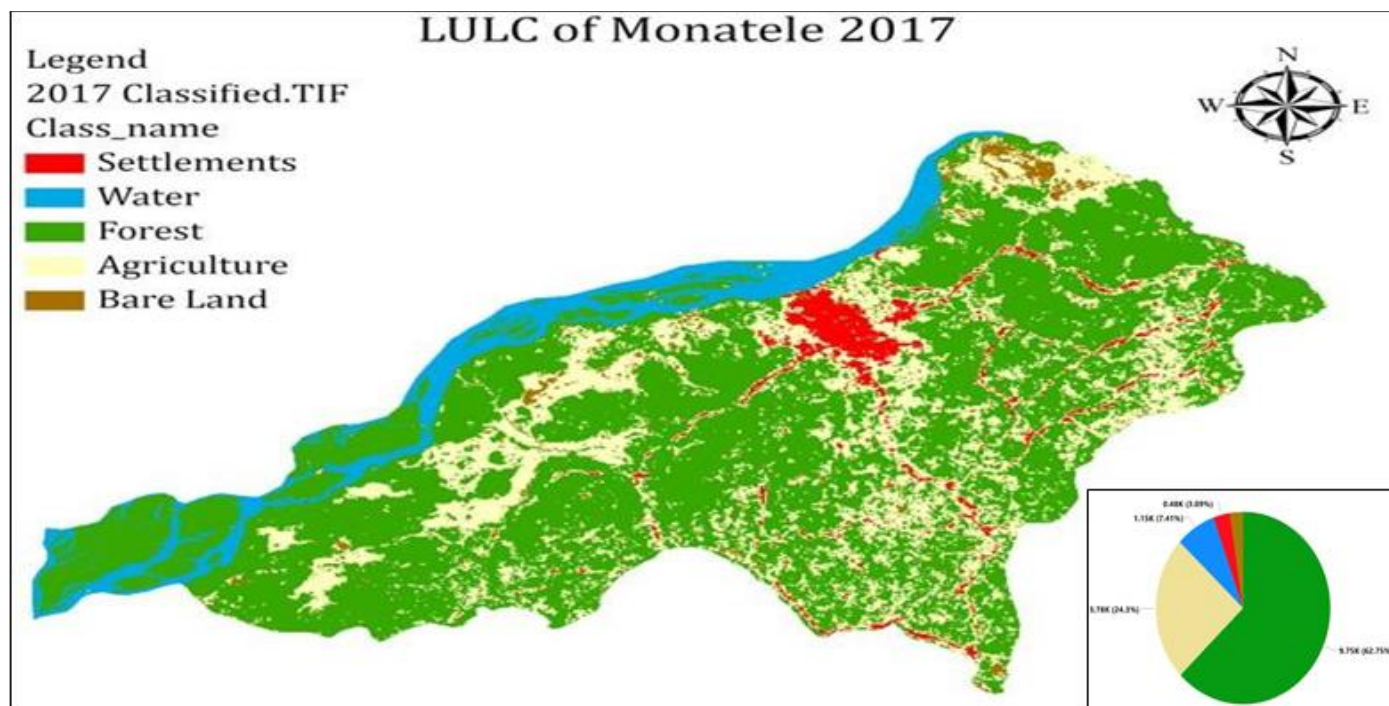


Fig 4 LULC of Monatéle in 2017

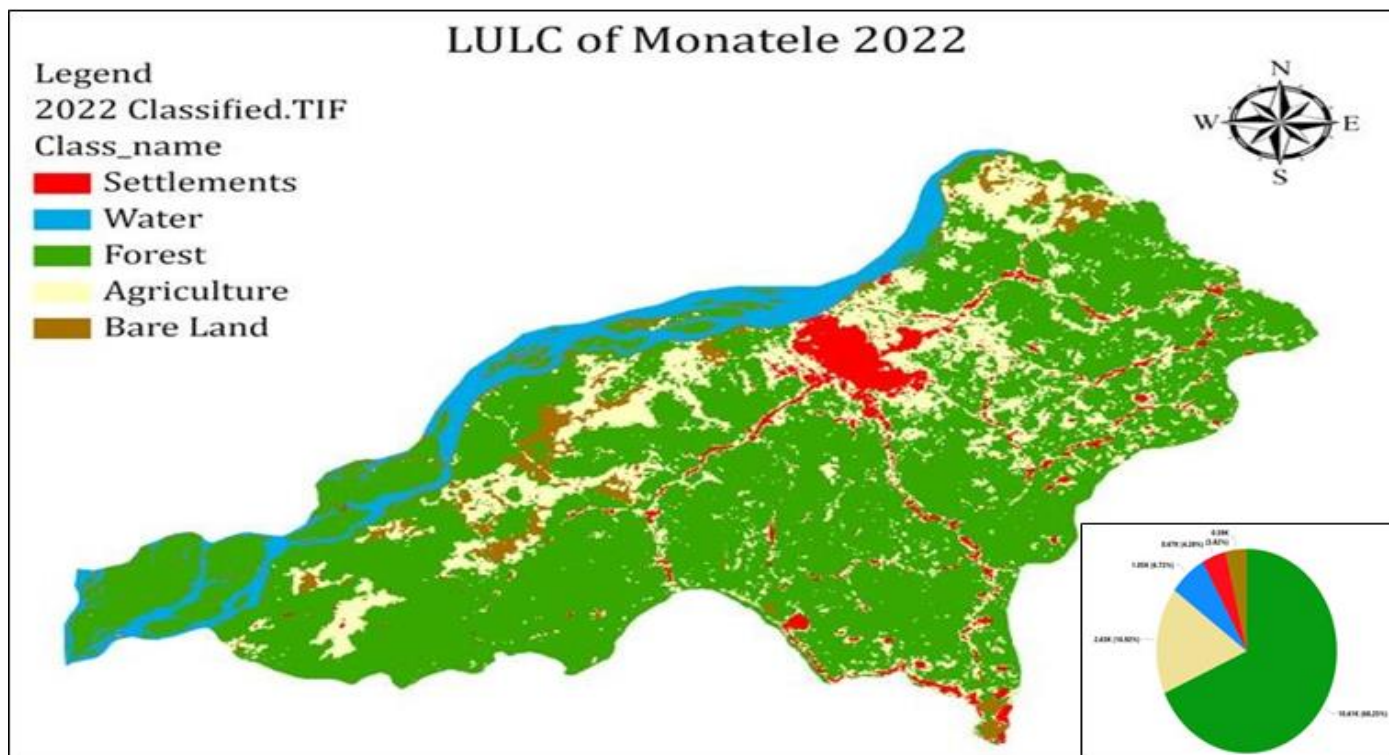


Fig 5 LULC of Monatéle in 2022

➤ Accuracy Assessments

Accuracy Assessment points were generated and compared based on the class values and sampled ground truthing, confusion matrices were generated, user's and producer's accuracies were calculated for each classification, overall accuracy and the Kappa coefficient were used to test and conclude on the classification accuracy. Overall accuracy is defined as the ratio between the total number of samples which are correctly classified and the total number of samples considered for the accuracy assessment. User's accuracy corresponds to error of

commission. It refers to the measurement of how many of the samples of a particular class matched correctly. On the other hand, producer's accuracy corresponds to errors of omission. It is a measure of how much of land in each LULC category was classified correctly. The Misclassification Matrices for the images of 2010, 2017 and 2022 in the tables below show overall accuracy of 0.90, 0.88 and 0.86 and Kappa coefficients of 0.82 (82%), 0.81 (81%) and 0.77 (77%) respectively which makes the classifications very good according to Moriasi et al., 2007.

Table 4 Confusion Matrix of 2010 Image Classification

ClassValue	C_10	C_20	C_30	C_40	C_50	Total	U_Accuracy	Kappa
C_10	8	0	2	0	0	10	0.8	0
C_20	0	9	1	0	0	10	0.9	0
C_30	2	2	66	4	0	74	0.89	0
C_40	0	0	1	11	0	12	0.92	0
C_50	0	0	0	0	10	10	1	0
Total	10	11	70	15	10	116	0	0
P_Accuracy	0.8	0.82	0.94	0.73	1	0	0.9	0
Kappa	0	0	0	0	0	0	0	0.82

LEGEND	C_10	Settlements
Class	C_20	Water
Producer Accuracy	C_30	Forest
User Accuracy	C_40	Agriculture
Overall Accuracy	C_50	Bare Land
Kappa Coefficient	U_Accuracy	User Accuracy
	P_Accuracy	producer's Accuracy

Table 5 Confusion Matrix of 2017 Image Classification

ClassValue	C_10	C_20	C_30	C_40	C_50	Total	U_Accuracy	Kappa
C_10	9	0	0	1	0	10	0.9	0
C_20	0	8	2	0	0	10	0.8	0
C_30	0	0	59	3	1	63	0.94	0
C_40	0	0	5	19	0	24	0.79	0
C_50	0	0	1	1	8	10	0.8	0
Total	9	8	67	24	9	117	0	0
P_Accuracy	1	1	0.88	0.79	0.89	0	0.88	0
Kappa	0	0	0	0	0	0	0	0.81











LEGEND		C_10	Settlements
	Class	C_20	Water
	Producer Accuracy	C_30	Forest
	User Accuracy	C_40	Agriculture
	Overall Accuracy	C_50	Bare Land
	Kappa Coefficient	U_Accuracy	User Accuracy
		P_Accuracy	Producer Accuracy

Table 6 Confusion Matrix of 2022 Image Classification

ClassValue	C_10	C_20	C_30	C_40	C_50	Total	U_Accuracy	Kappa
C_10	8	0	1	1	0	10	0.8	0
C_20	0	10	0	0	0	10	1	0
C_30	0	2	64	2	0	68	0.94	0
C_40	2	0	3	10	2	17	0.59	0
C_50	0	1	1	1	7	10	0.7	0
Total	10	13	69	14	9	115	0	0
P_Accuracy	0.8	0.77	0.93	0.71	0.78	0	0.86	0
Kappa	0	0	0	0	0	0	0	0.77

LEGEND		C_10	Settlements
	Class	C_20	Water
	Producer Accuracy	C_30	Forest
	User Accuracy	C_40	Agriculture
	Overall Accuracy	C_50	Bare Land
	Kappa Coefficient	U_Accuracy	User Accuracy
		P_Accuracy	Producer Accuracy

➤ *LULC Change Detection*

Change detection is one of the fundamental applications in imagery and remote sensing. It is the comparison of multiple raster datasets, typically collected for one area at different times, to determine the type, magnitude, and location of change. Change can occur because of anthropogenic activity, abrupt natural disturbances, or long-term climatological or environmental trends. The output from change detection is a difference raster where each pixel contains the type or magnitude of change. Change detection was done using ArcGIS Pro's Change Detection Wizard, and the net change between the classes was calculated for each the periods using the pixel value which was converted to the area by multiplying the area of each pixel by the square of the pixel resolution, as each pixel is squared from the raster information. The results of the LULC class change studies between 2010 and

2017 showed a net maximum variation in Agriculture Land, and a net minimum variation in Water. Agriculture increased to 95.36% (1843.45 Ha), Settlements increased by 92.16% (230.42 Ha), Bare land increased by 2.96% (10.93 Ha), Forest decreased by 14.94% (1712.86 Ha), while Water decreased by 24.40% (371.90 Ha). A change matrix was established to support the results by demonstrating which class change to which and with what probabilities. The results of the LULC class change studies between 2017 and 2022 showed a net maximum variation in Bare Land, and a net minimum variation in Agriculture Land. Bare Land increased to 56.31% (214.09 Ha), Settlements increased by 38.52% (18.09 Ha), Forest increased by 8.77% (854.76 Ha), Water decreased by 9.3% (107.15 Ha), while Water decreased by 30.37% (1146.83 Ha). A change matrix was established to support the results by demonstrating which class change to which and with what probabilities.

Table 7 Transition Matrix Showing LULC Change in Monatéle between 2010 and 2017

		2017										
2010	Area (Ha)	ST	WT	FR	AG	BL	Percentage	ST	WT	FR	AG	BL
	ST	216.4	0	5.83	21.78	6.01	ST	86.55	0	2.33	8.71	2.4
	WT	1.89	1125	375	12.73	9.56	WT	0.12	73.81	24.6	0.84	0.63
	FR	47.99	33.19	9026	2191	167	FR	0.42	0.29	78.73	19.11	1.46
	AG	178.9	1.91	380.5	1200	171.5	AG	9.25	0.01	19.68	62.09	8.87
	BL	22.84	0.41	101.8	231.4	12.92	BL	6.19	0.11	27.55	62.65	3.4

ST_Settlements, WT_Water, FR_Forest, AG_Agriculture, BL_Bare Land.

Table 8 Transition Matrix Showing LULC Change in Monatéle between 2017 and 2022

		2022										
2017	Area (Ha)	ST	WT	FR	AG	BL	Percentage	ST	WT	FR	AG	BL
	ST	228.51	0.09	1.49	19.37	0.56	ST	91.4	0.04	0.6	7.75	0.22
	WT	0.9	1475.7	5	0	42.62	WT	0.06	96.8	0.33	0	2.8
	FR	51.3	0.72	10822	469.4	120.87	FR	0.45	0	94.4	4.09	1.05
	AG	124.97	0.32	1433.6	38.83	335.95	AG	6.46	0.02	74.16	2	17.38
	BL	38.09	0	95.63	232.02	30.54	BL	9.61	0	24.13	58.55	7.71

ST_Settlements, WT_Water, FR_Forest, AG_Agriculture, BL_Bare Land.

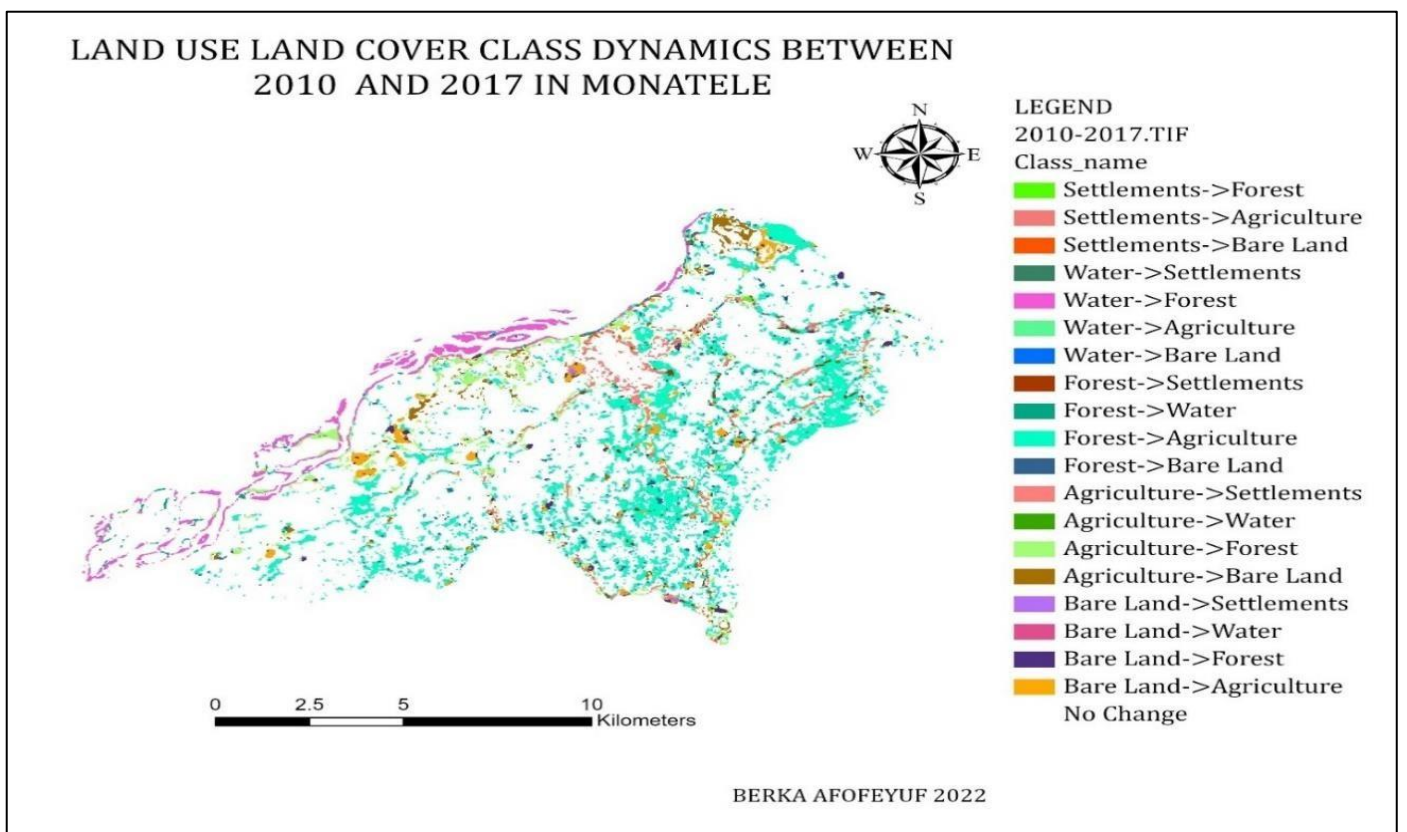


Fig 6 LULC Class Dynamics between 2010 and 2017

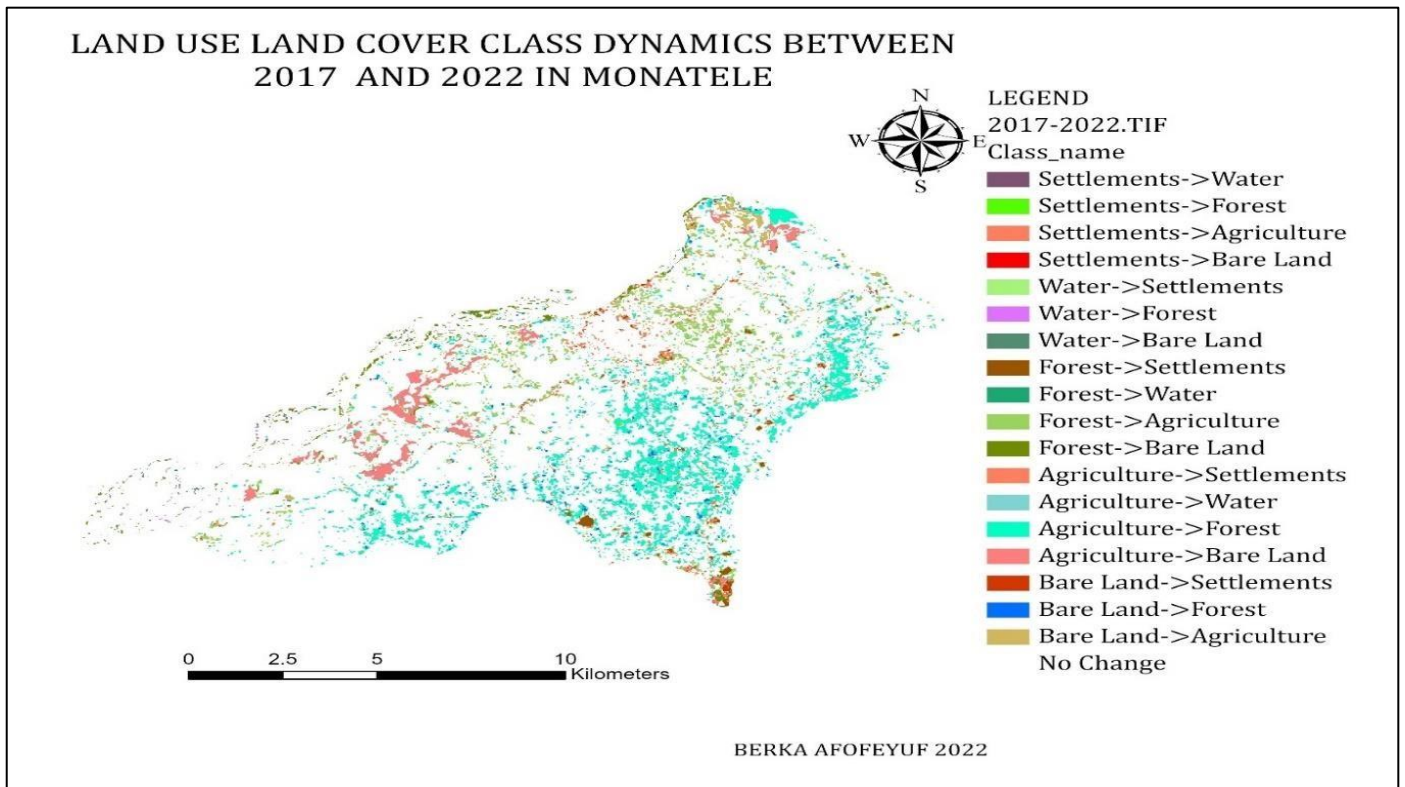


Fig 7 LULC Class Dynamics between 2017 and 2022

➤ Predictions

Using the LULC Maps of 2010 and 2017, a model prediction of 2022 was established and was used to determine the accuracy of the predictions for 2029 and 2035 using Relative Operating Characteristic (ROC) and Kappa indices. The validation results showed a correctness with Kappa for no information (Kno) 93.74%, Kappa for Location (Klocation) 96.15%, Kappa for location Stratum Level (KlocatioStrata) 96.15% and Kappa for Standard (Kstandard) 91.44%. These results show the high model capacity to simulate the 2029 and 2035 LULC patterns.

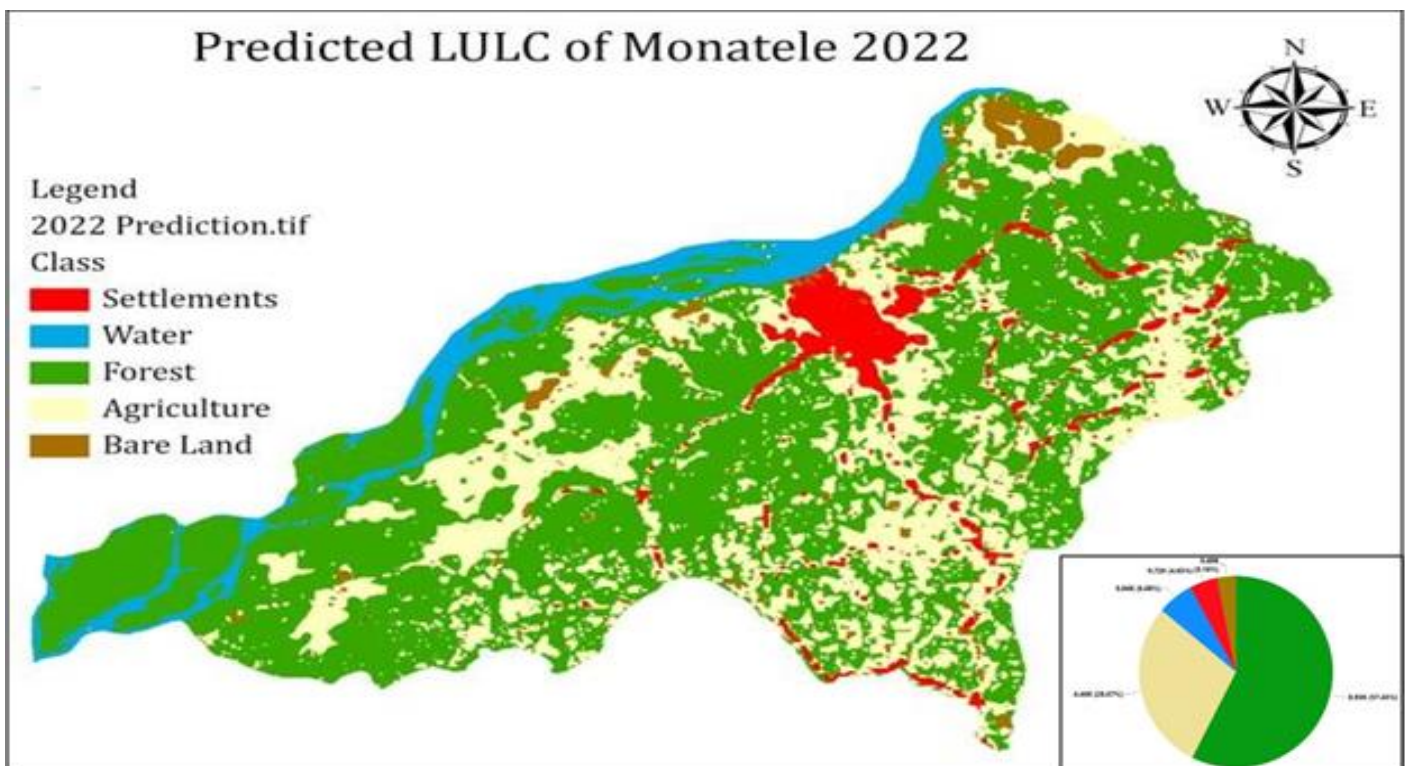


Fig 8 Predicted LULC of Monatéle 2022

For the simulations of the LULC maps of 2029 and 2035, change probability matrices were generated which represented the different class transition potentials, the LULC maps of 2010 and 2022 were used to get the Markovian transition areas which were used together with the Map of 2022 to perform these predictions.

Table 9 Transition Potential Probabilities for Transition from 2022 to 2029

	Settlements	Water	Forest	Agriculture	Bare Land
Settlements	0.8905	0	0.0099	0.0804	0.0192
Water	0.0018	0.8279	0.1656	0	0.0046
Forest	0	0.0021	0.8439	0.1497	0.0043
Agriculture	0.0681	0.0005	0.14	0.6962	0.0952
Bare Land	0.0287	0.0009	0.2065	0.608	0.1559

Table 10 Transition Potential Probabilities for Transition from 2022 to 2035

	Settlements	Water	Forest	Agriculture	Bare Land
Settlements	0.8084	0	0.0271	0.1371	0.0275
Water	0.0015	0.6993	0.295	0.0007	0.0035
Forest	0.0029	0.0036	0.7409	0.2343	0.0182
Agriculture	0.1083	0.001	0.2327	0.5741	0.0838
Bare Land	0.0682	0.0016	0.2897	0.5563	0.0842

According the predictions, in 2029, Forest will occupy 60.19% (9354.87 Ha), Agriculture will occupy 26.05% (4048.58 Ha), Settlements will occupy 5.74% (891.34 Ha), Water will occupy 5.33% (828.88 Ha), while Bare Land will occupy 2.69% (417.60 Ha). In 2035, Forest will occupy 61.22% (9515.07 Ha), Agriculture will occupy 25.19% (3914.26 Ha), Settlements will occupy 6.58% (1022.69 Ha), Water will occupy 4.58% (712.15 Ha), while Bare Land will occupy 2.43% (377.10 Ha) of the Commune of Monatélé.

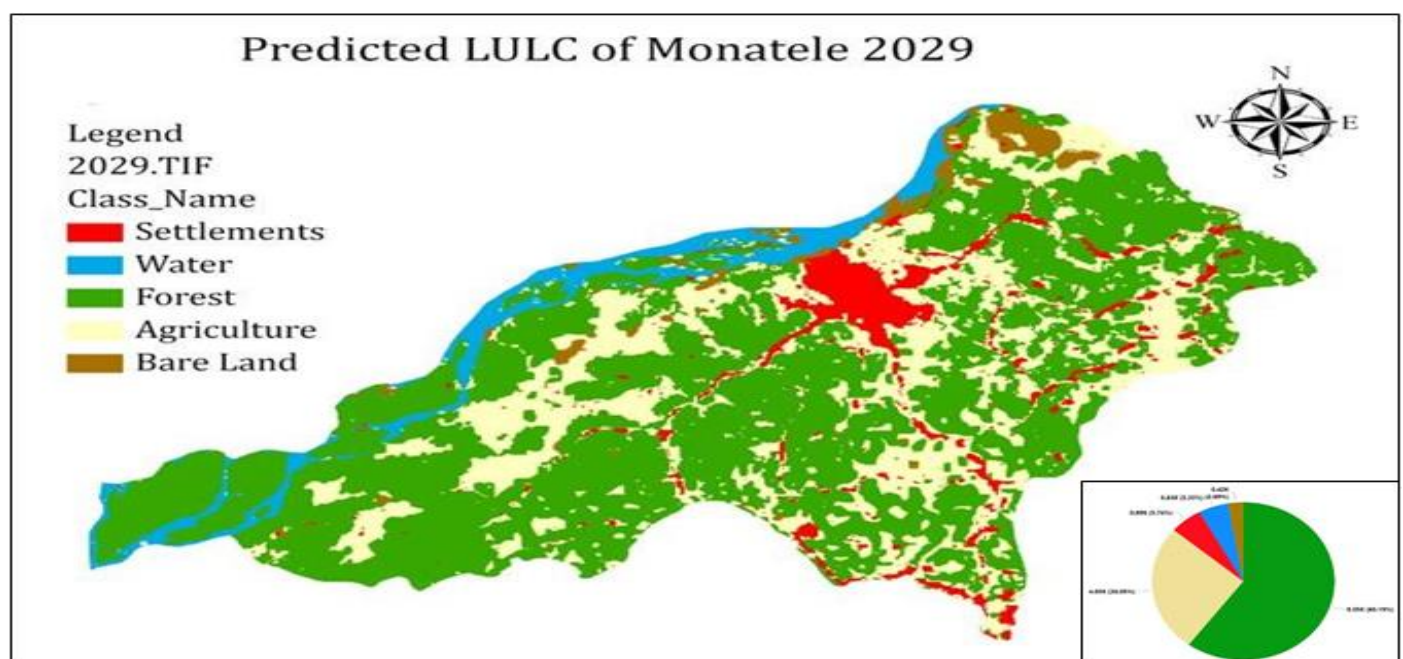


Fig 9 Predicted LULC of Monatélé 2029

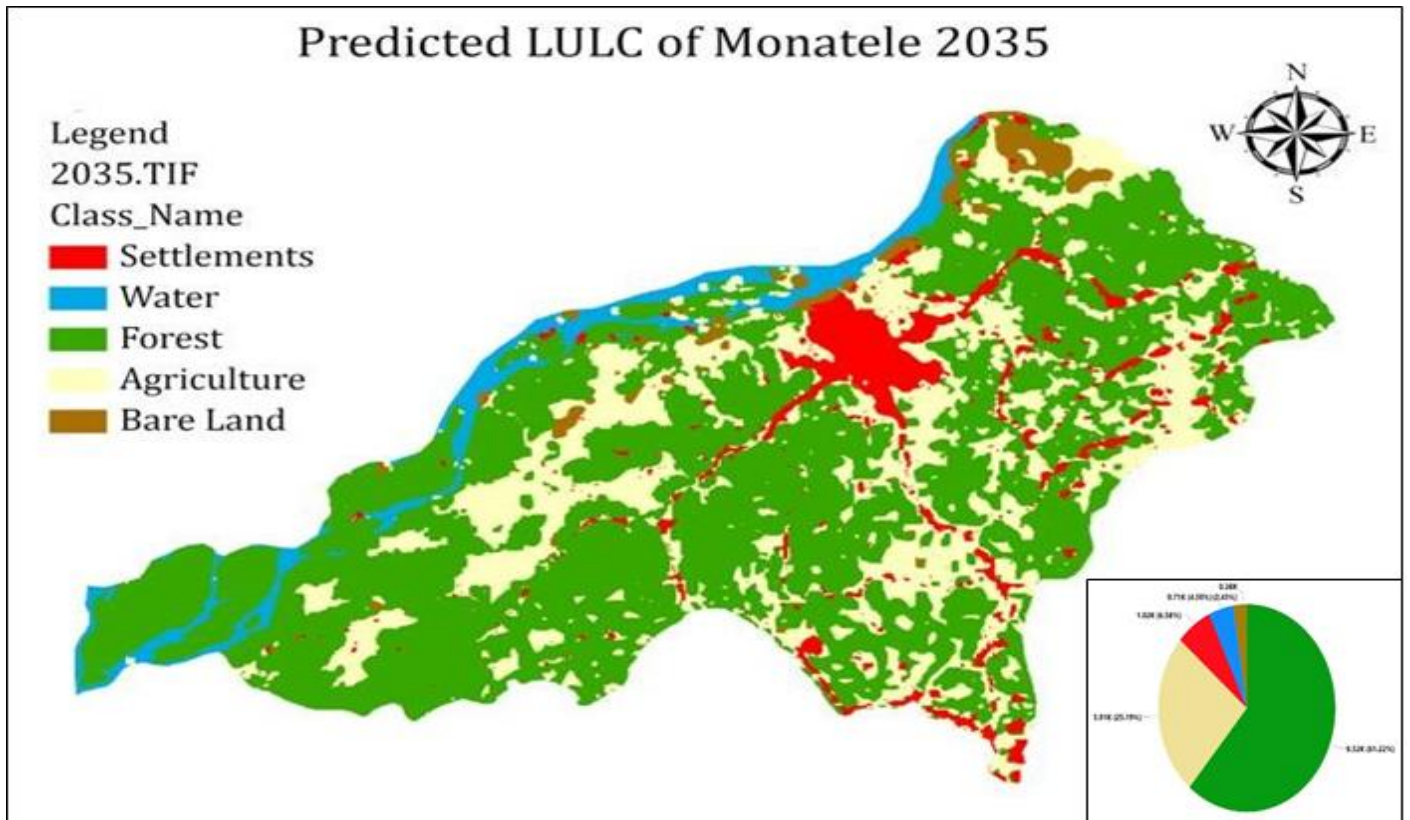


Fig 10 Predicted LULC of Monatéle 2035

These results show a net increase in settlements, a net decrease in water, a net decrease in Forest Land, an almost constant variation in Bare Land, and a net increase in Agriculture Land.

Table 11 Predicted Areas of Individual LULC Changes of 2029 and 2035

Year	LULC					
	2022 (Predicted)		2029		2035	
Class	Hectares	Percentage	Hectares	Percentage	Hectares	Percentage
Settlements	722.32	4.65	891.34	5.74	1022.69	6.58
Water	944.8	6.08	828.88	5.33	712.15	4.58
Forest	8928.5	57.45	9354.87	60.19	9515.07	61.22
Agriculture	4455.16	28.67	4048.58	26.05	3914.26	25.19
Bare Land	490.5	3.16	417.6	2.69	377.1	2.43
Total	15540.97	100	15540.97	100	15540.97	100

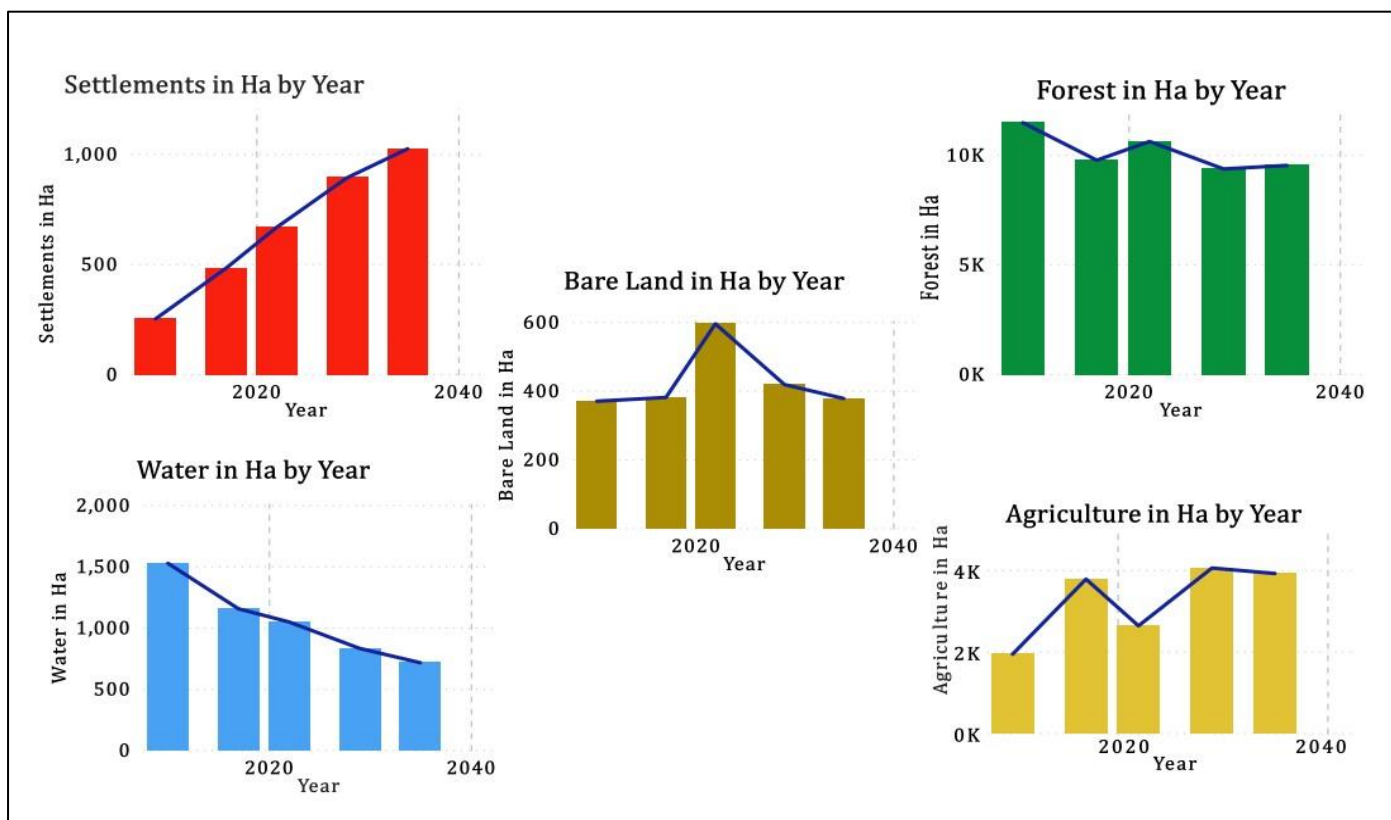


Fig 11 Line and Stacked Chart Showing Variation of Different Classes between 2010 and 2035

➤ *Significance of Results*

The results show a consistent increase in settlements, a consistent decrease in water mass, a net increase in agriculture and net this in forest and an almost constant variation in bare land. This growth in settlements will lead to uncontrolled urbanization and anarchy in the nearest future if appropriate measures are not put in place (town planning being the most effective), this will equally lead pollution of the environment, increase pressure on natural resources and consequent resource depletion, ecological degradation, increase demand in basic necessities and facilities such as portable water, electricity, schools, good transport systems, et cetera. However, controlled, this growth in settlement will lead to an increase in human capital, specialization, creativity, improved demographic structures et cetera. Monatélé having fishing as one of its main economic activities, producing about 60 tons of fish per year (Communal Development Plan of Monatélé), will experience a great loss in the years to come if measures are not taken to control the continual loss of water mass. A net decrease in forest implies a loss in biodiversity, a reduction in one of the main local economic activities which is tourism. Loss in forest also implies risk of floods, erosion, landslides, air pollution, irregularities in water cycles, damage of natural habitats, increase climate change and global warming, et cetera. Increasing agriculture land implies supporting livelihoods through food, increase in trade, local employment opportunities, reduction of grocery expenses, et cetera. Uncontrolled however, this increase will lead to deforestation, loss in biodiversity, soil and water contamination, et cetera. Recommendations have been made in the last section to tackle these issues.

IV. CONCLUSION

This study had as objective to elaborate the present LULC and give possible future predictions of the LULC of the subdivision of Monatélé in Cameroon, in order to help the decision makers in this subdivision make informed decisions based on past trends, present reality and future possibilities. In order to achieve this objective, a literature review was done, concepts of LULC were defined and understood, and two principal tools were settled on for use to achieve this course; GIS and remote sensing. A defined methodology for the work was equally established including the data acquisition (raster, vector files, field survey...) and processing, and simulation or prediction with all the tools possible (ArcGIS Pro, ERDAS 2022, QGIS, IDRISI Selva...). The application of the defined methodology, which classified the subdivision into five main classes, showed that in the subdivision of Monatélé in Cameroon, between 2010 and 2022, Settlements have increased, almost doubling between 2010 and 2017, Water has constantly been on the decrease with water area getting transform a lot into Forest, Agriculture Land has been on an increase, while Bare Land has also increase between 2010 and 2022. In numerical terms, Settlements increased from 1.61% in 2010 through 3.09% in 2017 to 4.28% in 2022, Water decreased from 9.81% in 2010 through 7.41% in 2017 to 6.72% in 2022, Forest decreased from 73.77% in 2010 to 62.75 in 2017 and then increased to 68.25 in 2022, Agriculture Land increased from 12.44% to 24.3% in 2017 and then decreased to 16.92% in 2022, accounting a lot for the increase in Forest, while Bare Land increased from 2.38% in 2010 through 2.45% in 2017 and 3.82% in 2022. Predictions

using the robust CA-Markov showed that in 2029 and 2035, settlements will occupy 5.74% and 6.58%, Water will occupy 5.33% and 4.58%, Forest will occupy 60.19% and 61.22%, Agriculture will occupy 26.05% and 25.19% while Bare Land will occupy 2.69% and 2.43% respectively. As an outcome, forest and water with high environmental content are greatly reducing. This is threatening to ecological values. Settlements and Agriculture are increasing at high rates and will continue to increase and need to be controlled. There arises to this effect a need for land use planning in Monatéle to avoid disorderly settlement patterns and reduce pressure on natural resources for sustainable development as is presently the case with most of the metropolitan cities of Yaoundé and Douala.

REFERENCES

- [1]. Abbas Taati, Fereydoon Sarmadian, Amin Mousavi, Chamran Taghati H. P., & Amir Hossein E. H. (2015, March). Land Use Classification using Support Vector Machine and Maximum Likelihood Algorithms by Landsat 5 TM Images. *Walailak Journal of Science and Technology (WJST)*, 12(8), 681-687. doi :10.14456/WJST.2015.33
- [2]. Drummond A. Mark, Roger F. Auch, Krista A. Kartensen, Kristi L. Saylor, Janis L. Taylor, & Thomas R. Loveland. (2012, July 12). Land change variability and human–environment dynamics in the United States Great Plains. *Land Use Policy*, 29(3), 710-723. doi: <https://doi.org/10.1016/j.landusepol.2011.11.007>
- [3]. El-Kawy O.R. Abd, Jan Ketil Rød, Hatiyah Ismail, & Ahmed Saeid Suliman. (2011, April). Land use and land cover change detection in the Western Nile Delta of Egypt using remote sensing data. *Applied Geography*, 31(2), 483-494. doi: [10.1016/j.apgeog.2010.10.012](https://doi.org/10.1016/j.apgeog.2010.10.012)
- [4]. Fan Fenglei, Weng Qihao, & Yunpeng Wang. (2007, July). Land Use and Land Cover Change in Guangzhou, China, from 1998 to 2003, Based on Landsat TM /ETM+ Imagery. *Sensors*, 7(7), 1323-1342. doi :10.3390/s7071323
- [5]. Fang Shoufan, Guangxing Wang, Alan B. Anderson, & George Z Gertner. (2006, February). The Impact of Misclassification in Land Use Maps in the Prediction of Landscape Dynamics. *Landscape Ecology*, 21(2), 233-242. doi :10.1007/s10980-005-1051-7
- [6]. Foley Jonathan, Ruth Defries, Gregory Asner, Peter Snyder, Navin Ramankutty, Iain Colin Prentice, . . . Chad Monfreda. (2005, August). Global Consequences of Land Use. *Science (New York, N.Y.)*, 309(5734), 570-4. doi:10.1126/science.1111772
- [7]. Foody, G. M. (2002, April). Status of land cover classification accuracy assessment. *Remote Sensing of Environment*, 80(1), 185-201. doi: [https://doi.org/10.1016/S00344257\(01\)00295-4](https://doi.org/10.1016/S00344257(01)00295-4)
- [8]. Garedew Efrem, Mats Sandewall, Ulf Söderberg, & Bruce Morgan Campbell. (2009, September). Land-Use and Land-Cover Dynamics in the Central Rift Valley of Ethiopia. *Environmental Management*, 44(4), 683-94. doi:10.1007/s00267-009-9355-z
- [9]. Gilani Hammad, Phuntsho Phuntsho, Basanta Shrestha, Him Lal Shrestha, Sudip Pradhan, Msr Murthy, & Berandra Badjracharya. (2014, March). Decadal land cover change dynamics in Bhutan. *Journal of Environmental Management*. doi: [10.1016/j.jenvman.2014.02.014](https://doi.org/10.1016/j.jenvman.2014.02.014)
- [10]. Houghton, R. A. (1994, May). The Worldwide Extent of Land-Use Change. *Biosciences*, 44(5), 305-313. Retrieved June 2023, from <https://www.jstor.org/stable/1312380>
- [11]. International Geosphere-Biosphere Program, International Human Dimensions Programme on Global Environmental Change. (1999). *Land-Use and Land-Cover Change (LUCC) Implementation Strategy*. Stockholm, Bonn: IHDP publication programme, Global Change News Letter. Retrieved June 2023, from <https://www.bing.com/ck/>
- [12]. J.G.P.W., Clevers. (2009). Russell G. Congalton and Kass Green, Assessing the Accuracy of Remotely Sensed Data—Principles and Practices (Second edition). *International Journal of applied Earth Observation and Geoinformation*, 11, 448-449. doi: <https://doi.org/10.1016/j.jag.2009.07.002>
- [13]. Jin Suming, Limin Yang, Patrick Danielson, Collin Homer, Joyce Fry, & George Xian. (2009, May 15). A comprehensive change detection method for updating the National Land Cover Database to circa 2011. *Remote Sensing of Environment*, 132, 159-175. doi: <https://doi.org/10.1016/j.rse.2013.01.012>
- [14]. José Antonio V. M., & Beatriz Elena A. A. (2019, March). Comparison of maximum likelihood, support vector machines, and random forest techniques in satellite images classification. *Tecnura*, 23(59), 3-10. doi :10.14483/22487638.14826
- [15]. Kogo B. Kipkemboi , Lalit Kumar, & Richard Koech. (2019, April). Analysis of spatio-temporal dynamics of land use and cover changes in Western Kenya. *Geocarto International*, 36(9), 1-16. doi :10.1080/10106049.2019.1608594
- [16]. Langat Philip, Lalit Kumar, Richard Koech, & Manoj K. Ghosh. (2019, August). Monitoring of Land Use/Land -Cover dynamics using remote sensing: A case of Tana River Basin, Kenya. *Geocarto International*, 36(12), 1-20. doi :10.1080/10106049.2019.1655798
- [17]. Lu D., & Q. Weng. (2007, March 17). A survey of image classification methods and techniques for improving classification performance. *International Journal of Remote Sensing*, 28(5), 823-870. doi : <https://doi.org/10.1080/01431160600746456>

- [18]. Mather R. John & Sdasyuk V. Galina. (1991, December). Global Change: Geographical Approaches. (J. E. Oliver, Ed.) Geographical Review, 83(1), 112-114. Retrieved June 2023, from <https://www.jstor.org/stable/215396>
- [19]. Moriasi D. N., Arnold J. G., Van Liew, M. W. Bingner, R. L. Harmel, & Veith T. L. (2007). Model Evaluation Guidelines for Systematic Quantification of Accuracy in Watershed Simulation. Transactions of ASABE, 50(3), 885-900. doi: <https://doi.org/10.13031/2013.23153>
- [20]. Muriithi, F. K. (2016, May). Land use and land cover (LULC) changes in semi-arid sub watersheds of Laikipia and Athi River basins, Kenya, as influenced by expanding intensive commercial horticulture. Remote Sensing Applications : Society and Environment, 3, 73-88. doi : <https://doi.org/10.1016/j.rsase.2016.01.002>
- [21]. Prenzel, B. (2004, May). Remote sensing-based quantification of land-cover and land-use change for planning. Progress in Planning, 61(4), 281-299. doi:10.1016/S03059006(03)00065-5
- [22]. Prisley S. P., & Smith J. L. (1987, September). Using classification error matrices to improve the accuracy of weighted land-cover models. Photogrammetric Engineering and Remote Sensing, 53(9), 1259 – 1263. doi : WOS : A1987J981900010
- [23]. Tchindjang Mesmin, Saha Frédéric, Voundi Eric, Mbevo Fendoung Philippes, Ngo Makak Rose, Issan Ismaël, & Tchoumbou Frédéric Sédrick. (2020). Land Use and Land Cover Changes in the Centre Region of Cameroon. Preprints, 2020020264. Retrieved June 2023
- [24]. Turner Billie, William Meyer, & David L. Skole. (1994, January 01). Global land-use/land-cover change: towards an integrated study. Ambio 23 (1), 91-95. Retrieved June 2023, from <https://typeset.io/papers/global-land-use-land-cover-change-towards-an-integrated1d9mzzdm31>
- [25]. Fopa Kenne D. M. (2018). Télédétection pour L'évaluation et la simulation Géo prospective de la croissance Urbaine : Cas de la ville de Yaounde
- [26]. BALLA NGO NGUIDJOE M. V. (2020). Apport des Images Satellitaires dans l'étude de L'évolution Spatio-Temporel de l'occupation de sol de la ville de Douala.